Molecular Cell
Article

The miR-17-92 MicroRNA Cluster Regulates Multiple Components of the TGF-β Pathway in Neuroblastoma

Pieter Mestdagh,[1,11] Anna-Karin Boström,[2,11] Francis Impens,[3,4,11] Erik Fredlund,[1,5,6] Gert Van Peer,[1] Pasqualino De Antonellis,[7] Kristoffer von Stedingk,[2] Bart Ghesquière,[3,4] Stefanie Schulte,[8] Michael Dews,[9] Andrei Thomas-Tikhonenko,[9] Johannes H. Schulte,[8] Massimo Zollo,[7,10] Alexander Schramm,[8] Kris Gevaert,[3,4] Håkan Axelson,[2] Frank Speleman,[1,12] and Jo Vandesompele[1,12,*]

[1]Center for Medical Genetics, Ghent University Hospital, B-9000 Ghent, Belgium
[2]Department of Laboratory Medicine, Center for Molecular Pathology, Lund University, SE-205 02 Malmo, Sweden
[3]Department of Medical Protein Research, VIB, B-9000 Ghent, Belgium
[4]Department of Biochemistry, Ghent University, B-9000 Ghent, Belgium
[5]Department of Oncology, Clinical Sciences, Lund University, SE-205 02 Malmo, Sweden
[6]CREATE Health, Strategic Centre for Translational Cancer Research, Lund University, SE-205 02 Malmo, Sweden
[7]Centro di Ingegneria Genetica e Biotecnologia Avanzate (CEINGE), 80131 Naples, Italy
[8]University Hospital of Essen, 45147 Essen, Germany
[9]Division of Cancer Pathobiology, Department of Pathology & Laboratory Medicine, The Children's Hospital of Philadelphia Research Institute and University of Pennsylvania School of Medicine, Philadelphia, PA 19104, USA
[10]Dipartimento di Biochimica e Biotecnologie Mediche (DBBM), Università di Napoli, 80131 Naples, Italy
[11]These authors contributed equally to this work
[12]These authors contributed equally to this work
*Correspondence: joke.vandesompele@ugent.be
DOI 10.1016/j.molcel.2010.11.038

SUMMARY

The miR-17-92 microRNA cluster is often activated in cancer cells, but the identity of its targets remains elusive. Using SILAC and quantitative mass spectrometry, we examined the effects of activation of the miR-17-92 cluster on global protein expression in neuroblastoma (NB) cells. Our results reveal cooperation between individual miR-17-92 miRNAs and implicate miR-17-92 in multiple hallmarks of cancer, including proliferation and cell adhesion. Most importantly, we show that miR-17-92 is a potent inhibitor of TGF-β signaling. By functioning both upstream and downstream of pSMAD2, miR-17-92 activation triggers downregulation of multiple key effectors along the TGF-β signaling cascade as well as direct inhibition of TGF-β-responsive genes.

INTRODUCTION

MicroRNAs (miRNAs) belong to a regulatory class of small noncoding RNAs with a fundamental role in numerous aspects of cell biology, such as cell-cycle regulation, apoptosis, differentiation, and maintaining stemness (reviewed in Bartel [2004]). Only 20–25 nucleotides (nt) in length, miRNAs function as key molecules in the posttranscriptional repression of gene expression. Upon miRNA assembly in the RNA-induced silencing complex (RISC), binding between the miRNA seed (nt 2–7 counted from the 5′ end of the miRNA) and complementary sites in the 3′ untranslated region (3′UTR) of target mRNAs results in degradation of the mRNA or inhibition of translation (reviewed in Bartel [2009]). Based on the 3′UTR site context, algorithms predict that up to 60% of all coding genes are under the control of one or more miRNAs (Friedman et al., 2009). However, these predictions suffer from a high degree of false positives, and to date, only a fraction of miRNA-mRNA interactions have been experimentally validated.

In cancer, miRNAs function both as oncogenes or tumor suppressors (reviewed in Calin and Croce [2006]; Esquela-Kerscher and Slack [2006]). Some of these miRNAs were identified as essential components of known cancer pathways, such as the p53-induced miR-34 family (He et al., 2007; Raver-Shapira et al., 2007) or the c-MYC/MYCN-induced miR-17-92 cluster (O'Donnell et al., 2005). The oncogenic miR-17-92 cluster consists of six individual miRNAs (miR-17, miR-18a, miR-19a, miR-19b, miR-20a, and miR-92a) located within a polycistronic transcript on human chromosome 13. Gene duplications and deletions eventually resulted in two miR-17-92 paralogs, the miR-106b-25 cluster on chromosome 7 and the miR-106a-363 cluster on chromosome X. Of these clusters, miR-17-92 is the most frequently activated one in cancer. miRNA expression profiling studies revealed miR-17-92 overexpression, both in hematopoietic malignancies (such as B cell lymphomas [He et al., 2005]) and solid tumors (including breast, colon, and lung cancer [Castellano et al., 2009; Hayashita et al., 2005; Lanza et al., 2007]) and neuroblastoma (NB) (Mestdagh et al., 2009a). Overexpression can result from amplification of the miR-17-92 locus (He et al., 2005) or direct miR-17-92 transactivation by c-MYC/MYCN (Dews et al., 2010; Fontana et al., 2008; Mestdagh et al., 2009a; O'Donnell et al., 2005). The oncogenic nature of miR-17-92 activation is supported by the identification of

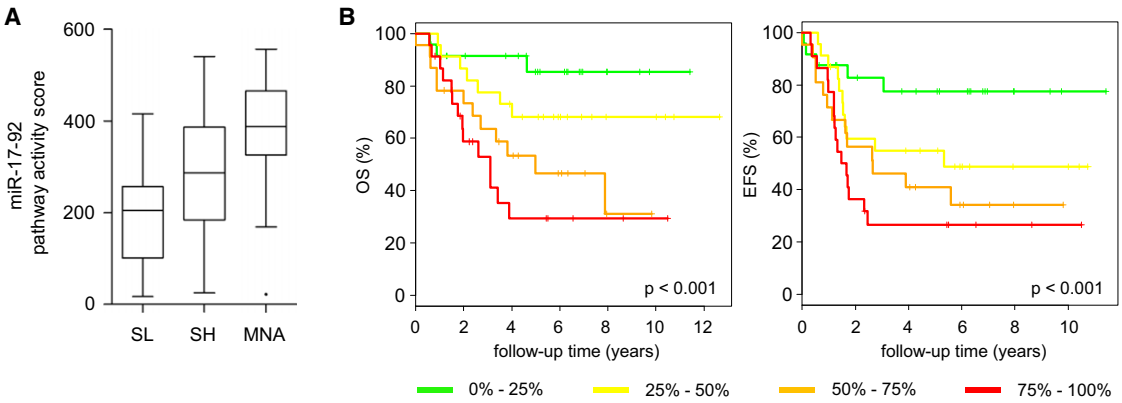

Figure 1. miR-17-92 Cluster Activation Is a Marker for Poor Prognosis

(A) miR-17-92 pathway activity is scored in three clinicogenetic subsets of NB tumors (data set D1, Table S1), *MYCN* amplified tumors (MNA), *MYCN* single copy high-risk tumors (SH), and *MYCN* single-copy low risk tumors (SL) (whiskers: Tukey). miR-17-92 pathway activity score is significantly higher in MNA versus SH (Mann Whitney, $p < 0.05$), MNA versus SL ($p < 0.0001$), and SH versus SL ($p < 0.01$).

(B) Kaplan Meier plots for overall (OS) and event free survival (EFS) based on the pathway activity score of miR-17-92, represented as quartiles. Increased activity of miR-17-92 is proportionally correlated to both poor overall and event-free survival.

miR-17-92 targets with key roles in cell-cycle control and cell death. In particular, miR-17 and miR-20a target the cyclin-dependent kinase inhibitor CDKN1A (p21), a negative regulator of the G_1-S transition (Fontana et al., 2008), and miR-17 targets the proapoptotic BCL2L11 (Bim) (Fontana et al., 2008). In gastric cancer, downregulation of p21 by the miR-17 and miR-20a paralogs miR-106b and miR-93 renders the cells insensitive to TGF-β-induced cell-cycle arrest whereas miR-25 (a miR-92a paralog) inhibits TGF-β-dependent apoptosis through the repression of BCL2L11 (Petrocca et al., 2008).

Thus far, the number of identified miR-17-92 targets remains relatively limited, thus precluding a comprehensive understanding of the full oncogenic potential of this miRNA cluster. In a first step toward this goal, we examined the effects of miR-17-92 cluster activation on the proteome of NB cancer cells. Using quantitative mass spectrometry, we analyzed the response of thousands of proteins upon miR-17-92 activation in NB cells. NB is an excellent model to study the effects of miR-17-92 activation because high-risk NB tumors are characterized by increased MYCN/c-MYC activity either through *MYCN* amplification or increased *c-MYC* expression, both resulting in elevated miR-17-92 levels (Mestdagh et al., 2009a). Our results demonstrate that miR-17-92 is implicated in multiple hallmarks of the tumorigenic program, including proliferation and cell adhesion. Most importantly, we dissect the role of miR-17-92 as a potent inhibitor of TGF-β-signaling acting on multiple levels along the signaling cascade.

RESULTS

miR-17-92 Cluster Activation Is a Marker for Poor Survival

In NB, miR-17-92 expression is activated through direct MYCN/c-MYC promoter binding (Fontana et al., 2008; Mestdagh et al., 2009b). We quantified miR-17-92 expression on a cohort of 95 primary untreated NB tumor samples (data set D1, Table S1; GEO accession number GSE21713) (Mestdagh et al., 2009a). The activation of the entire miR-17-92 cluster was evaluated by means of a pathway activity score (Fredlund et al., 2008; Mestdagh et al., 2009a). NB tumors were divided into three cohorts, *MYCN* single copy low-risk tumors (SL), *MYCN* single copy high-risk tumors (SH), and *MYCN* amplified tumors (MNA). The miR-17-92 pathway activity was highest in the MNA tumors, followed by the SH tumors and the SL tumors (Figure 1A). Each individual miRNA is upregulated in the MNA samples suggesting that the entire miR-17-92 cluster, rather than a subset of miRNAs, is of potential relevance (Mann Whitney, $p < 0.05$) (Figure S1A). We next evaluated miR-17-92 pathway activation with respect to NB patient survival. Kaplan-Meier analysis demonstrated that miR-17-92 activity was proportional to overall and event-free survival (log rank, $p < 0.001$), underscoring the importance of miR-17-92 activation in NB tumor biology (Figure 1B). Except for miR-19b, expression of the other miRNAs within the miR-17-92 cluster showed similar correlations (Figure S1B).

Impact of miR-17-92 Activation on Protein Output

To study the regulatory effects of miR-17-92 activation, quantitative mass spectrometry was applied to measure protein response in a cellular model (SHEP-TR-miR-17-92) with tetracycline-inducible miR-17-92 expression (Mestdagh et al., 2009a). This approach provides the most relevant readout as it directly measures the impact of a miRNA on protein output (Baek et al., 2008; Selbach et al., 2008). Average miR-17-92 induction upon tetracycline treatment was in the range of miR-17-92 fold changes between MNA and SL tumors (Figure S2A) (data not shown). Profiling of 430 miRNAs revealed no significant effects on global miRNA expression suggesting that miR-17-92 induction does not affect the processing of other miRNAs (data not shown). SHEP-TR-miR-17-92 cells were differentially labeled using SILAC (stable isotope labeling with amino acids in cell culture) (Ong et al., 2002) and then either treated with tetracycline for 72 hr or left untreated, followed by methionine COFRADIC

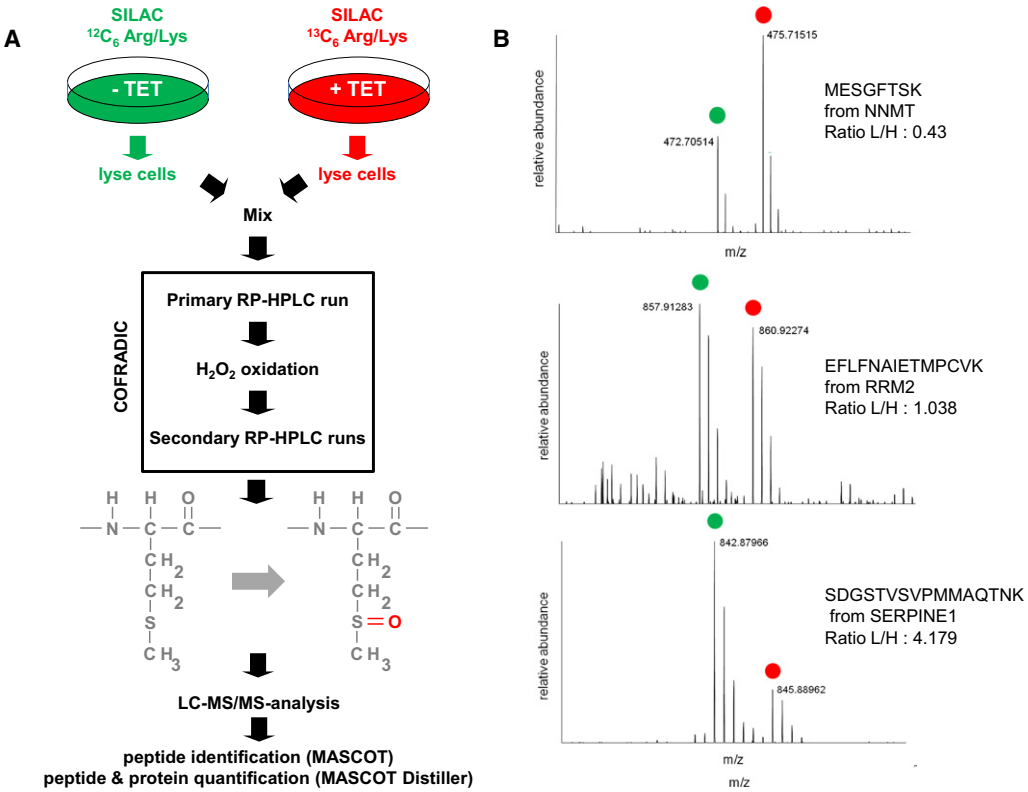

Figure 2. Analysis of Global Protein Expression upon miR-17-92 Activation

(A) Tetracycline treated (+TET) and untreated (−TET) SHEP-TR-miR-17-92 cells were metabolically labeled using SILAC. Methionine-containing peptides were isolated using COFRADIC technology and subsequently analyzed using LC-MS/MS.

(B) Representative LC-MS/MS spectra for an upregulated protein (NNMT), unchanged protein (RRM2), and downregulated protein (SERPINE1).

isolation of methionyl peptides (Gevaert et al., 2002) and identification of these peptides by LC-MS/MS (Figure 2A). Only proteins that were quantified by at least two different peptides over two different proteome analyses (n = 3249) were selected for further analysis (Colaert et al., 2010). Most proteins were in fact quantified by more than two peptides (Figure S3B). Differential protein expression was determined as the average protein ratio of the differentially labeled fractions across the biological replicates (Table S2; Figures 2B and S3C). Based on a fold-change expression cutoff of 0.5 $\log_2$ units (see Supplemental Information for cutoff definition), 144 proteins were downregulated upon miR-17-92 activation.

To assess whether the measured protein response reflects regulatory miR-17-92 effects, we performed an unbiased search for all possible 7-mer motifs (n = 16,384) in the 3′UTR of the downregulated proteins (15th percentile) and compared these to motif occurrence in the 3′UTR of the remaining proteins. We found seven motifs to be overrepresented in the 3′UTR of the downregulated proteins, with the five most significant motifs belonging to the miR-17-92 miRNAs: miR-17, miR-19a, miR-19b, miR-20a, and miR-92a (Fisher Exact, $p < 0.05$, Bonferoni multiple testing correction) (Figure 3A). Strikingly, there was no enrichment for miR-18a seeds, suggesting that miR-18a does not substantially contribute to protein repression upon miR-17-92 activation. Analyses using the 20th percentile gave similar results (data not shown). Analyses for the 5′UTR and coding sequence (CDS) did not reveal significant enrichments for miR-17-92 miRNA seed sequences. However, we did observe an enrichment for the 7-mer-m8 seed of miR-17* in the CDS of the downregulated proteins, suggesting that miR-17*-mediated protein repression might depend on CDS binding.

To evaluate miR-17-92 seed efficiency with respect to protein repression, we plotted the cumulative distribution of protein fold changes for proteins with at least one miR-17-92 3′UTR 6-mer, 7-mer-A1, 7-mer-m8, or 8-mer seed and compared these to proteins without miR-17-92 seeds (Figure 3B). As expected, protein repression was highest in the presence of an 8-mer seed (Kolmogorov-Smirnov, $p = 2.20 \times 10^{-16}$) followed by 7-mer-m8 ($p = 1.11 \times 10^{-6}$), 7-mer-A1 ($p = 0.00011$) and 6-mer seeds ($p = 0.0027$). When evaluating each miR-17-92 miRNA separately, we observed similar results for miR-17/miR-20a, miR-19a/miR-19b, and miR-92a (miR-17/mir-20a and miR-19a/miR-19b were analyzed together as they share identical seeds) (Figure 3C). For miR-18a, the relation between seed occurrence and protein fold change was less pronounced, further supporting our observation that the contribution of miR-18a to miR-17-92-mediated protein repression is limited.

The fraction of proteins containing at least one miR-17-92 7-8-mer seed was highest for proteins that were downregulated at least 2-fold (82%) and decreased to background levels (45%)

A

motif	miRNA	seed	p-value*
GCACTTT	miR-17, miR-20a	7mer-m8	2.4×10^{-12}
TTTGCAC	miR-19a, miR-19b	7mer-m8	4.0×10^{-9}
TTGCACA	miR-19a, miR-19b	7mer-A1	1.7×10^{-8}
GTGCAAT	miR-92a	7mer-m8	5.5×10^{-8}
CACTTTA	miR-17, miR-20a	7mer-A1	8.7×10^{-8}
AGCACTT	miR-302, miR-372, miR-373, miR-520	7mer-m8	1.8×10^{-7}
CCTCCAG	NA	NA	1.92×10^{-6}

* Fisher's Exact p-value

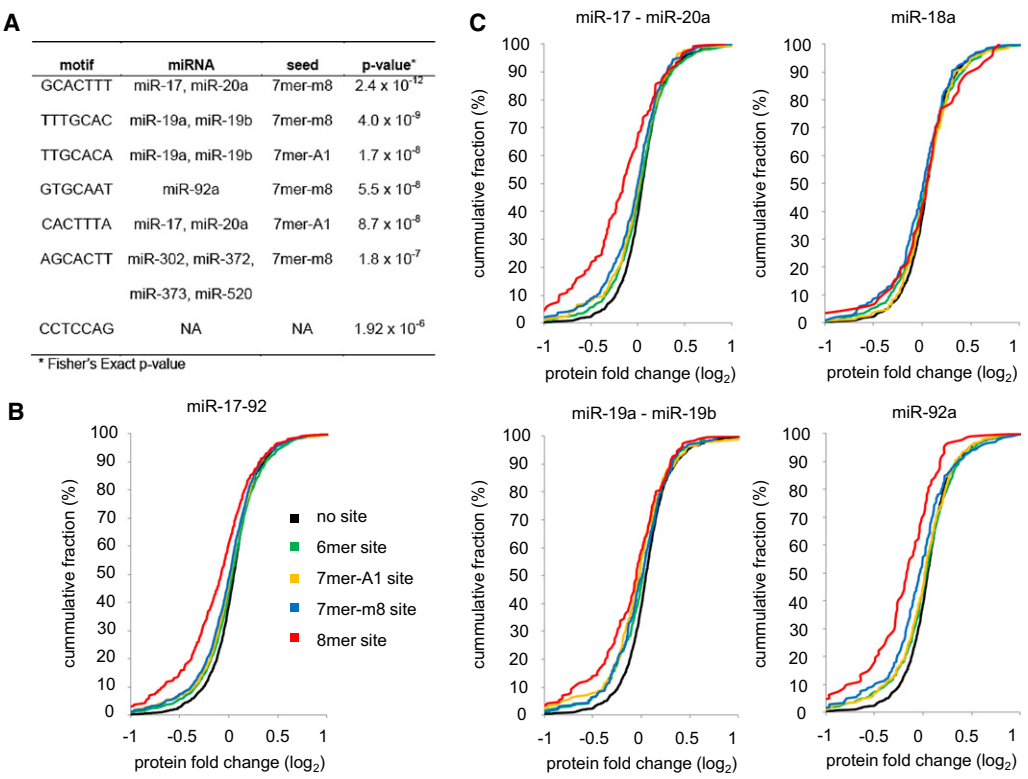

Figure 3. miR-17-92 Activation Induces Widespread Repression of Targeted Proteins

(A) Overview of all significantly enriched heptamer motifs in the 3′UTR of transcripts from repressed proteins. The top five significantly enriched motifs correspond to miR-17-92 target sites. One motif corresponds to the 7-mer-m8 seed of the miR-302/miR-372 family, which differs in only one base with the 7-mer-m8 seed of miR-17/miR-20a. The last motif did not correspond to any known miRNA nor did it show any overlap with miR-17-92 seeds.

(B) The cumulative distribution of protein fold changes upon miR-17-92 activation, calculated for five different protein subsets: proteins with at least one miR-17-92 8-mer site (red), 7-mer-m8 site (blue), 7-mer-A1 site (yellow), 6-mer site (green), and no site (black).

(C) Identical analysis as in (B) but for each individual miRNA from the miR-17-92 cluster. The miR-17/miR-20a and the miR-19a/miR-19b were analyzed together as they share identical seeds.

for unchanged proteins (Figure S3A). Robust protein repression was also characterized by the presence of multiple miR-17-92 3′UTR sites per protein (Figure S3B), suggesting that individual miR-17-92 miRNAs cooperate to achieve target repression. This correlation was only observed for 3′UTR sites and not for 5′UTR or CDS sites (Figures S3C and S3D). To further evaluate miRNA cooperation, we analyzed co-occurrence of individual miR-17-92 sites in the 3′UTR of downregulated proteins and compared this to co-occurrence in the 3′UTR of upregulated proteins (used as a reference control set). We identified significant co-occurrence for miR-17/miR-20a sites and miR-19a/miR-19b sites confirming cooperation between individual miRNAs (Figure S3E). miR-18a sites almost never occurred in the absence of other miR-17-92 sites (8.33%) and were significantly associated with miR-17/miR-20a sites (Figure S3E).

miR-17-92 Affects Multiple Cancer Pathways

To gain insight into the pathways affected by oncogenic miR-17-92 activation, we performed gene set enrichment analysis (GSEA) (Subramanian et al., 2005) using all measured proteins, ranked according to their fold change. Thirty-six gene sets were significantly enriched in the positive phenotype (i.e., downregulated proteins) while nine were enriched in the negative phenotype (i.e., upregulated proteins). Of the latter, six were related to increased metabolic activity of the mitochondrial oxidative phosphorylation energy production pathway (Figure S4). In NB, miR-17-92 expression is activated by MYCN/c-MYC transcription factors that have been shown to regulate genes involved in the biogenesis of mitochondria and metabolism (Zhang et al., 2007). Our results now provide evidence that this, at least in part, is mediated through miR-17-92 activation.

The contribution of each individual miRNA to the significant gene lists in the positive phenotype was calculated and visualized as a heatmap (Figure 4A). Among the gene lists enriched in the positive phenotype, which reflect direct miR-17-92-regulated pathways, we identified multiple cancer-related processes such as cell proliferation, cell adhesion, TGF-β signaling, estrogen-signaling, and RAS signaling (Figure 4A). Hierarchical clustering reveals a close association between miR-17/miR-20a- and miR-19a/miR-19b-regulated pathways, reflecting the previously observed co-occurrence of these sites. Again, miR-18a clusters further away from the remaining miR-17-92 miRNAs and is characterized by weak gene list associations.

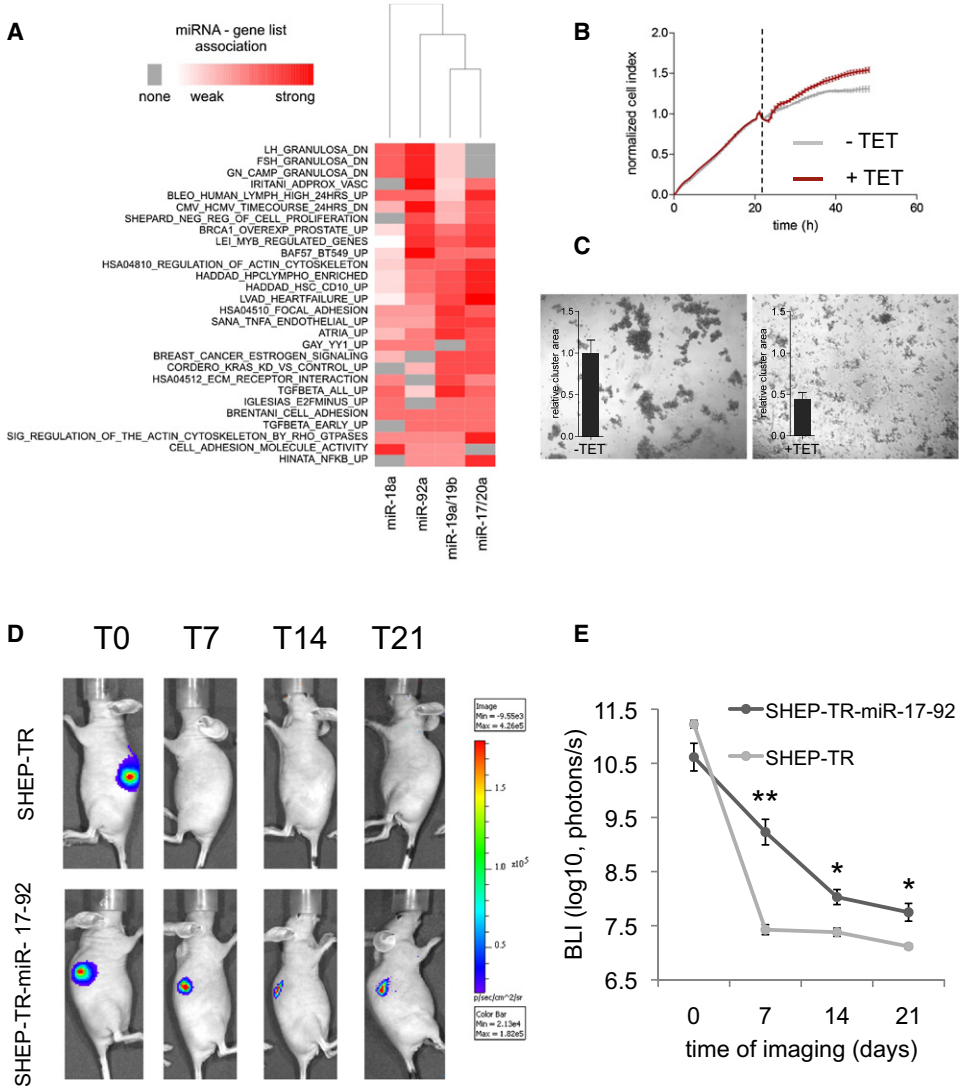

Figure 4. miR-17-92 Activation Regulates Multiple Cancer Pathways

(A) Heatmap of significant miRNA-pathway associations, identified through gene set enrichment analysis. The intensity of the association is based on the fraction of genes with at least one 7-mer or 8-mer 3′UTR site.

(B) Normalized cell index (mean ± standard deviation) as a measure for proliferation of tetracycline treated (+TET) and untreated (−TET) SHEP-TR-miR-17-92 cells. Treatment was initiated 20 hr post seeding.

(C) Evaluation of the cell-cell adhesion of tetracycline treated and untreated SHEP-TR-miR-17-92 cells. Measurements of the relative cluster area for three independent experiments using ImageJ are displayed as bar plots. Upon miR-17-92 activation, the area of the clusters dropped by >50% resulting in more but smaller aggregates.

(D) Representative analyses of bioluminescence imaging (BLI) of luciferase positive SHEP-TR-miR-17-92 and SHEP-TR cells injected etherotopically and subcutaneously in the right and left flank of nude athymic mice. Bar scale color indicates the number of photons/s measured by IVIS 3D imaging instrumentation. SHEP miR17-92 cells in vivo are still alive after 21 days post cell subcutaneous implantation.

(E) Bioluminescence imaging (BLI) of luciferase positive SHEP-TR-miR-17-92 and SHEP-TR cells injected etherotopically and subcutaneously in the right and left flank of nude athymic mice. Luciferase signals were measured at 0, 7, 14, and 21 days postengraftment and are shown as the mean ± SEM of five mice. Significant differences between SHEP-TR and SHEP-TR-miR-17-92 cells are indicated by * (Student t test, $p < 0.05$) and ** (Student t test, $p < 0.01$).

In NB, the oncogenic nature of miR-17-92 has been ascribed to its ability to promote cell proliferation through the regulation of CDKN1A and BCL2L11 (Fontana et al., 2008). GSEA results indicate that miR-17-92 has a much broader influence and targets different oncogenic pathways. As a proof of concept, we tried to validate the association with increased proliferation and decreased cell adhesion in the SHEP-TR-miR-17-92 cells. Cell proliferation was evaluated in real-time using the xCELLigence system. Upon miR-17-92 activation, proliferation of SHEP-TR-miR-17-92 cells increased (Figure 4B) and intercellular cell adhesion significantly decreased (Figure 4C). To evaluate the effect of miR-17-92 activation in vivo we performed

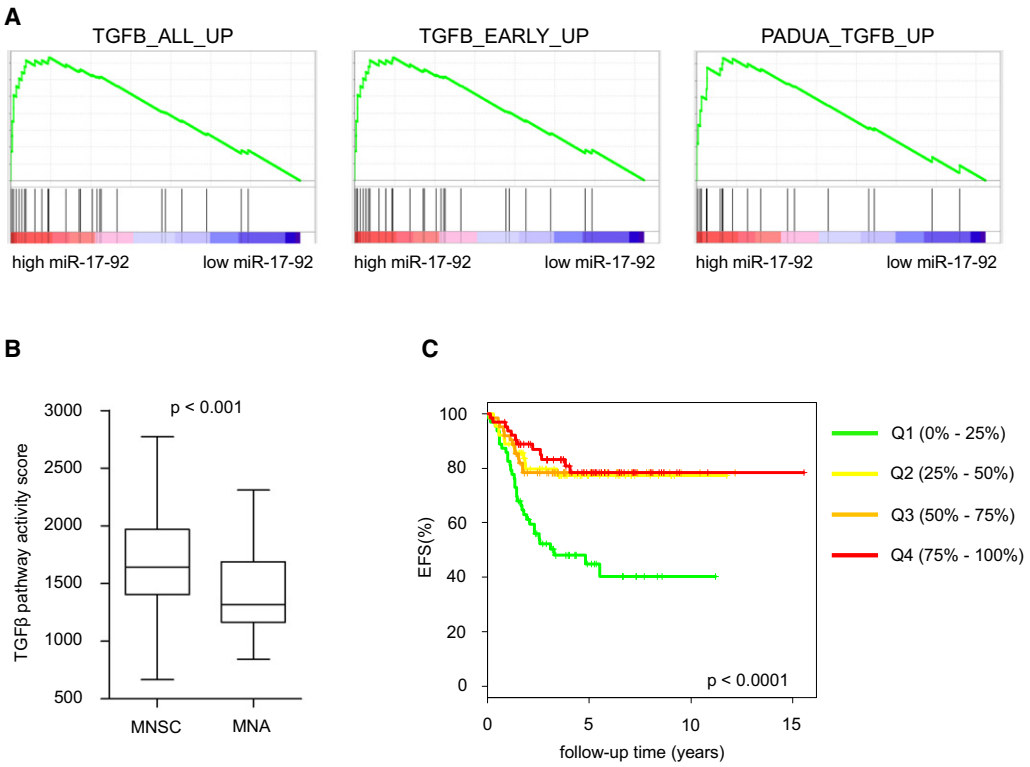

Figure 5. miR-17-92 Activation Represses the TGF-β Pathway

(A) Gene set enrichment analysis plots for three different TGF-β gene sets showing significant enrichment among the miR-17-92 repressed proteins.

(B) TGF-β pathway activity score in *MYCN* amplified NB tumors (MNA) and *MYCN* single-copy NB tumors (MNSC) (data set D2, Table S1). MNA tumors show significantly lower TGF-β pathway activity (Mann Whitney, $p < 0.001$) (whiskers: Tukey).

(C) Kaplan Meier plot for event free survival (EFS) based on the TGF-β pathway activity score, represented as quartiles (dataset D2, Table S1). Increased activity of miR-17-92 is proportionally correlated to event-free survival.

etherotopic injection of SHEP-TR-miR-17-92 and SHEP-TR (control) cells in the right and left flanking site, respectively, of atymic nude mice that were given tetracyclin and visualized tumor cells using bioluminescence imaging. For SHEP-TR cells, the luciferase signal dropped to background levels after 7 days of engraftment, which is in line with previous findings demonstarting that SHEP cells are not tumorigenic in vivo (Schweigerer et al., 1990) (Figures 4D and 4E). In contrast, SHEP-TR-miR-17-92 cells persisted much longer and showed statistically higer luciferase signals at 7, 14, and 21 days, indicating that, although tumorigenesis decreases, miR-17-92 activation significantly prolongs the engraftment of SHEP cells, probably through increased proliferation and decreased apoptosis, activities previously ascribed to miR-17-92 overexpression (Fontana et al., 2008). Together, these results confirm the relation between miR-17-92 activation and cell proliferation and reveal a role for miR-17-92 in the regulation of cell adhesion, hereby confirming the GSEA results.

miR-17-92 Impairs TGF-β Activity

GSEA analysis identified three TGF-β-responsive gene sets (Padua et al., 2008; Verrecchia et al., 2001) among the proteins downregulated upon miR-17-92 activation in the SHEP-TR-miR-17-92 cells (Figure 5A). To exclude the possibility that repression of TGF-β-responsive genes is an artifact of miRNA overexpression, we analyzed eight published protein expression data sets of miRNA overexpression (Baek et al., 2008; Selbach et al., 2008) using GSEA. None of the TGF-β gene lists were significantly enriched in any of the data sets, suggesting the observed effect to be related to miR-17-92. For a subset of the TGF-β-responsive genes, the measured protein repression was confirmed on the mRNA level using RT-qPCR (Figure S5). We next evaluated this TGF-β signature in NB tumor samples using the pathway activity score of all genes that significantly contributed to the GSEA results ($n = 21$). For this purpose, we used the larger Oberthuer data set (Oberthuer et al., 2006) (data set D2, Table S1) to increase the power of our analysis. TGF-β pathway activity was significantly downregulated in MNA NB tumors that are characterized by high miR-17-92 expression (Mann Whitney, $p < 0.001$) (Figure 5B), and showed a negative correlation to MYC pathway activity (Spearman's Rank $p < 0.01$, rho = −0.460). In addition, Kaplan-Meier survival analysis indicates that tumors with low TGF-β pathway activity are characterized by poor event-free survival (log-rank, $p < 0.0001$) (Figure 5C). To further substantiate the inverse relation between TGF-β target gene expression and miR-17-92 expression, we performed an expression correlation analysis in a subset of 40 of the 95 NB tumors for which also mRNA expression was

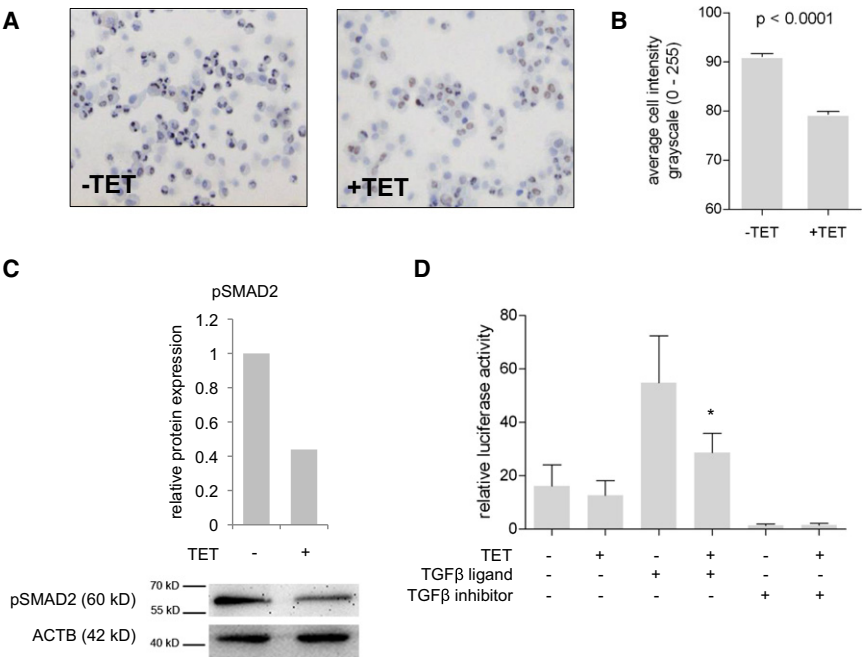

Figure 6. miR-17-92 Inhibits pSMAD2 Levels and Activity

(A and B) Immunohistochemical detection of phosphorylated SMAD2 protein (pSMAD2) in tetracycline treated (+TET) and untreated (−TET) SHEP-TR-miR-17-92 cells. The cell intensity measurement (mean ± SEM) reveals a significant decrease in pSMAD2 levels in tetracycline treated cells (Mann Whitney, $p < 0.0001$).

(C) Western blot analysis indicates a strong decrease (2.3-fold) in pSMAD2 levels upon miR-17-92 induction (+TET).

(D) The relative luciferase activity of a pSMAD2 reporter construct (mean ± SEM). Activation of miR-17-92 expression through tetracycline treatment (+TET) results in a significant (*) decrease in reporter activity after stimulation of the TGF-β pathway with TGF-β1 (TGF-β ligand). TGF-β-inhibitor treatment completely abrogates the reporter activity.

available (data set D3, Table S1) (Mestdagh et al., 2009a). Hierarchical clustering of the correlation coefficients revealed that, indeed, miR-17-92 expression inversely correlates to TGF-β target gene expression (Figure S6A). These results confirm that TGF-β signaling is downregulated in aggressive NB tumors with high miR-17-92 expression and underscore the potential importance of TGF-β activity in NB tumor biology.

We next evaluated which components of the TGF-β signaling cascade are controlled by miR-17-92 miRNAs. One important effector of active TGF-β signaling is phosphorylated SMAD2 protein (pSMAD2) that translocates to the nucleus to induce gene transcription. Upon tetracycline treatment of SHEP-TR-miR-17-92 cells, we observed a significant decrease in nuclear pSMAD2 levels (Mann Whitney, $p < 0.0001$) (Figures 6A–6C). A similar decrease was observed for pSMAD3 levels (data not shown). When SHEP-TR-miR-17-92 cells were transfected with a plasmid containing a SMAD-regulated luciferase reporter ($[CAGA]_{12}$-Luc) and treated with TGF-β1, a strong activation of the reporter gene was observed (Figure 6D). However, when miR-17-92 expression was activated through tetracycline treatment, reporter gene activation was substantially attenuated (Mann Whitney, $p < 0.001$) (Figure 6D). When the SHEP-TR-miR-17-92 cells were cultured in the presence of the potent TGFBR1 inhibitor SB431542 (Laping et al., 2002), the SMAD reporter gene activity was completely abrogated (Figure 6D). These results suggest that miR-17-92 activation impairs the TGF-β signaling cascade by acting upstream of pSMAD2.

miR-17-92 Affects Multiple Levels of the TGF-β Pathway

As decreased pSMAD2 levels are either caused by reduced receptor activity or reduced SMAD2 expression, we quantified *TGFBR2* and *SMAD2* mRNA expression in the SHEP-TR-miR-17-92 cells. Both *TGFBR2* and *SMAD2* expression levels decreased by at least 1.5-fold upon miR-17-92 activation (Figure 7A). *SMAD4*, the binding partner of pSMAD2, also displayed a decrease in expression upon miR-17-92 activation (Figure 7A). This negative correlation with miR-17-92 expression could be confirmed in primary NB tumor samples for *SMAD2* and *TGFBR2* (Spearman's Rank, $p < 0.01$) (Figure 7B), suggesting that miR-17-92 regulates their expression. Indeed, both genes contain miR-17-92 binding sites in their 3′UTR and a direct interaction between TGFBR2 and miR-20a has been established (Volinia et al., 2006). This miR-17-92 mediated silencing of TGFBR2 ultimately results in decreased pSMAD2 levels and decreased transcription of the TGF-β-target genes. In total, we identified 13 TGF-β-target genes to be downregulated on the protein level with a $\log_2$ fold change < -0.5 (7 out of 20 proteins in the PADUA_TGFB_UP gene set, 3 out of 16 proteins from the TGFB_EARLY_UP gene set, and 7 out of 28 proteins from the TGFB_ALL_UP gene set) (Table S3). As ten of these genes harbor miR-17-92 binding sites in their 3′UTR (Table S3), we wondered whether they might also be targeted directly by miR-17-92. To exclude the effects of miR-17-92 directed inactivation of TGF-β signaling on the expression of TGF-β-responsive genes, we first treated SHEP-TR-miR-17-92 cells for 4 hr with the TGFBR1 inhibitor SB431542, which completely abrogates TGF-β signaling (Figure 6C). Cells were subsequently treated with tetracycline to activate miR-17-92 expression and harvested at 24 hr and 48 hr after tetracycline treatment. From the six genes that were evaluated, three (*CDKN1A*, *ITGA4*, and *SERPINE1*) were downregulated after 24 hr of TGF-β-inhibitor treatment (t test, $p < 0.05$), confirming that they are regulated by TGF-β (Figure 7C). The remaining three genes (FNDC3B, ICAM1, and THBS1) did not show any differential expression after 24 hr; however, FNDC3B and THBS1 did respond to TGF-β-inhibitor treatment after 48 hr (data not shown). This suggests that, in NB, these are either not or indirectly responsive to TGF-β signaling (Figure 7D). Upon miR-17-92 activation, the TGF-β-responsive genes were further downregulated (t test, $p < 0.001$) (Figure 7C),

supporting our hypothesis that miR-17-92 also influences the expression of these genes, independent of its ability to inactivate TGF-β signaling. As expected, the genes that were not responsive to TGF-β inhibition did show decreased expression upon miR-17-92 activation (t test, $p < 0.001$) (Figure 7D).

To investigate which specific miRNAs contribute to the repression of the TGF-β-pathway, we overexpressed each miRNA from the miR-17-92 cluster separately and measured the expression of TGF-β-pathway components and target genes. Interestingly, we found that each miRNA contributes to the repression of one or more genes from the TGF-β pathway, suggesting that the entire miR-17-92 cluster, rather than a subset of miRNAs, mediates the repression of TGF-β signaling in NB cells (Figure S6B). Downregulation ($\log_2$ fold change < -0.5) upon miRNA transfectection was almost exclusively observed for those genes harboring a 3′UTR seed site for the respective miRNA (Fisher Exact, $p < 0.001$).

We next evaluated whether the miR-17-92-induced downregulation of TGF-β-pathway components is caused by direct binding between miR-17-92 miRNAs and miR-17-92 seed sites in the 3′UTR of TGFBR2, SMAD2, and SMAD4. To this purpose, DLD1DICER^{hypo} cells were transfected with 3′UTR luciferase reporter plasmids in combination with a pre-miR negative control or a miR-17-92 pre-miR for which one or multiple seed sites were present in the 3′UTR of the respective genes. We identified a direct interaction between *TGFBR2* and miR-17/20, *SMAD2* and miR-18a, and *SMAD4* and miR-18a, as evidenced by the significant decrease in luciferase activity compared to the pre-miR negative control (t test, $p < 0.01$, Figure 7E). Other putative miR-17-92 sites in the 3′UTR of *TGFBR2* (miR-19a/miR-19b), *SMAD2* (miR-19a/miR-19b, miR-92a), and *SMAD4* (miR-19a/miR-19b) did not affect luciferase signals (data not shown). Mutagenesis of the active miRNA seed sites resulted in a significant rescue of the luciferase signal (t test, $p < 0.01$), suggesting that the observed effects depend on the presence of the 3′UTR seed site. These results confirm *TGFBR2* as a direct miR-17-92 target gene and identify two additional TGF-β-pathway components, *SMAD2* and *SMAD4*, as miR-17-92 target genes.

To assess the importance of TGF-β-pathway inhibition in the proliferation phenotype observed upon miR-17-92 activation, we overexpressed SMAD2 and SMAD4 in the presence of activated miR-17-92. SMAD2/SMAD4 overexpression resulted in a 25% decrease in cell growth (t test, $p < 0.05$), indicating that miR-17-92 accelerated proliferation is, at least in part, depending on the downregulation of the TGF-β pathway. The relatively modest decrease in cell growth is probably explained by the fact that miR-17-92 directly regulates TGF-β target genes in a SMAD2/SMAD4 independent manner.

In conclusion, our data demonstrate that miR-17-92 activation triggers a targeted clampdown of TGF-β signaling by acting on multiple key effectors along the signaling cascade, as well as through the direct inhibition of TGF-β-responsive genes, hereby repressing the cytostatic effects of active TGF-β signaling (Figure S7).

DISCUSSION

Transcriptional activation of the miR-17-92 miRNA cluster by MYC/MYCN transcription factors occurs in multiple tumor entities, including NB (Hayashita et al., 2005; Mestdagh et al., 2009a; O'Donnell et al., 2005). Although the oncogenic nature of miR-17-92 activation is well established, the underlying targets and signaling cascades that are deregulated remain largely elusive. In addition, studies aimed at determining miR-17-92 targets have focused on individual members of the cluster, despite the observation that the entire cluster is activated (Mestdagh et al., 2009b; O'Donnell et al., 2005). Here, we have used an unbiased proteomics approach to identify miR-17-92 targeted pathways in a NB tumor model. Direct quantitative measurement of protein expression is preferred over the more straightforward mRNA profiling as a high-throughput method for miRNA target identification (Baek et al., 2008; Selbach et al., 2008).

Computational analysis of miR-17-92 seeds in the 3′UTR of transcripts from proteins supported the expected enrichment of direct miR-17-92 targets within the list of downregulated proteins detected using mass spectrometry. Moreover, a proportional relationship between seed frequency and fold downregulation was noted. This relationship not only holds for multiple seeds from an individual miR-17-92 miRNA but also for multiple seeds from different miR-17-92 miRNAs, suggesting cooperation between individual miRNAs from the cluster toward target protein repression. miR-17-92 miRNAs have indeed been shown to function in a cooperative and additive manner among others in the regulation of PTEN by miR-17 and miR-19 (Xiao et al., 2008). Our results further indicate that miR-19a/miR-19b and miR-17/miR-20a sites significantly co-occur in the 3′UTR of transcripts from several downregulated proteins. As these co-occurring sites were not observed for every possible combination of individual miR-17-92 miRNAs, we hypothesize that in NB, the miRNA components of the miR-17-92 cluster can regulate target expression either individually or in certain combinations with additive effects. However, miR-17-92 function might be highly context and cell-type specific as miR-19 was shown to be both necessary and sufficient to promote MYC-induced lymphomagenesis in the Eμ-myc mouse B cell lymphoma model (Olive et al., 2009).

While the fraction of downregulated proteins was enriched for seeds of miR-17/miR-20a, miR-19a/miR-19b, and miR-92a, enrichment for the miR-18a seed was not detected. Strikingly, miR-18a seeds rarely occur as the only seed(s) in the 3′UTR of a downregulated target and showed little or no correlation to protein fold change. Although this suggests that miR-18a is not substantially contributing to target deregulation, it does not imply that miR-18a lacks functionality, as miR-18a has been shown to regulate important cancer genes such as CTGF in colon cancer and estrogen receptor-α (ESR1) in NB (Dews et al., 2006; Lovén et al., 2010). Interestingly, we found miR-18a to regulate both SMAD2 and SMAD4, two key components of the TGF-β-signaling cascade, suggesting that miR-18a substantially contributes to pathway deregulation by regulating a selected set of target genes.

When all cluster components were combined, we identified a large number of targeted proteins belonging to diverse cancer-related pathways. Notably, estrogen receptor signaling was also among the targeted pathways. The fact that we identified such a wide variety of functions in NB cells suggests that miR-17-92 pleiotropy is not only related to different targets in different cell

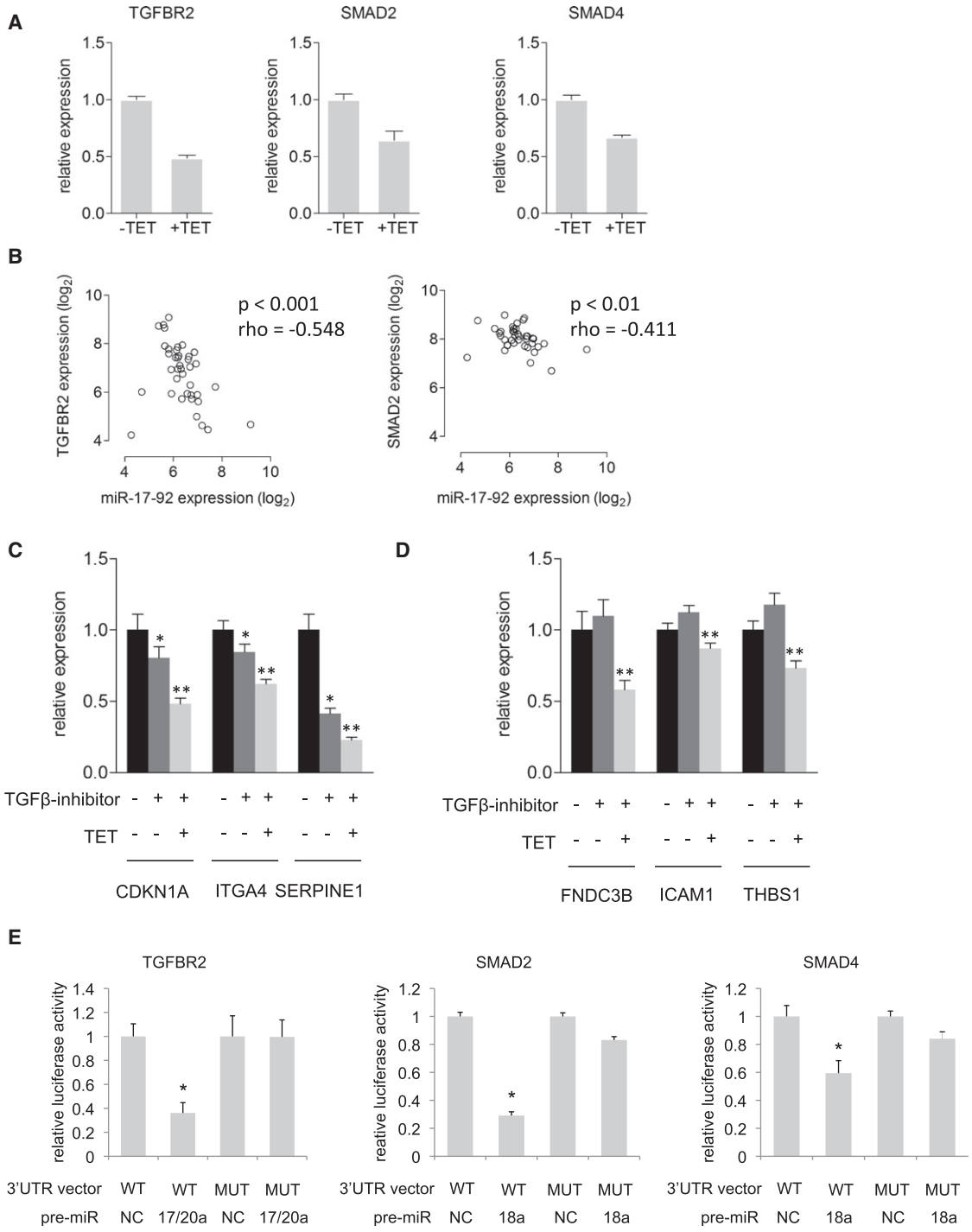

Figure 7. miR-17-92 Targets Multiple Components of the TGF-β Pathway

(A) The relative mRNA expression of TGF-β-responsive genes in tetracycline treated (+TET) and untreated SHEP-TR-miR-17-92 cells (+TET) (mean ± SEM).

(B) Significant negative correlation between TGFBR2 mRNA expression and miR-17-92 expression and SMAD2 mRNA expression and miR-17-92 expression in primary NB tumors. Spearman's rank rho-values and p values are listed.

(C and D) The relative mRNA expression (mean ± SEM) of a representative set of genes responsive to TGF-β (C) and genes not or (indirectly) responsive to TGF-β (D) in SHEP-TR-miR-17-92 cells that were either untreated, treated with TGF-β inhibitor, or treated with TGF-β inhibitor followed by miR-17-92 activation with tetracycline (TET) for 24 hr. In (C), genes respond to TGF-β-inhibitor treatment (t test, $p < 0.05$, indicated by *) and show an additional decrease in expression upon combined TGF-β-inhibitor treatment and miR-17-92 activation (t test, $p < 0.001$, indicated by *). In (D), genes only respond to mR-17-92 treatment (t test, $p < 0.001$, indicated by **).

types but also occurs within cell types. The molecular basis for this observation likely lies within the multiple components of the cluster and the complex interplay between them.

mir-17-92-directed regulation of the TGF-β-responsive genes *CDKN1A* and *BCL2L11* in NB cells has been described previously (Fontana et al., 2008). In gastric cancer, members of the miR-106b-25 cluster have also been shown to target *CDKN1A* and *BCL2L11* (Petrocca et al., 2008). Here we comprehensively demonstrate that miR-17-92 dampens TGF-β signaling in a multifaceted way by acting both upstream and downstream of pSMAD2/SMAD4, further underscoring its ability to regulate multiple components of the same pathway. This ability to simultaneously target the components of the signaling cascade, as well as the downstream effectors through multiple miRNAs, allows for tight control of the TGF-β-transcriptional program. Moreover, it offers the cells enormous flexibility and plasticity for regulation of different subsets of TGF-β target genes. In NB, enhanced TGF-β signaling, through increased TGFBR2 expression, results in reduced cell growth in vitro and disables the ability of the cells to form tumors in vivo (Turco et al., 2000). Instead, cells assume a terminally differentiated neuronal phenotype and display increased expression of axonal growth-associated protein (GAP43) and neurofilaments (Turco et al., 2000). Treatment of NB cells with TGF-β1 induces a similar phenotype (Scarpa et al., 1996). In addition, retinoic acid (RA) induces differentiation of NB cells, known to downregulate MYCN, accompanied by the increased expression of TGF-β1, TGFBR1, TGFBR2, and TGFBR3, resulting in the induction of a negative autocrine TGF-β1 growth regulatory loop (Cohen et al., 1995). We have shown that aggressive NB tumors evade the cytostatic TGF-β pathway through miR-17-92 directed targeting of key components of the pathway as well as downstream effectors. Reactivation of TGF-β signaling through miR-17-92 inhibition could be a promising therapeutic approach, as it would not only result in reactivation of TGFBR2 expression but also relieve the direct miR-17-92-mediated repression of TGF-β-responsive genes.

EXPERIMENTAL PROCEDURES

Cell Culture

SHEP-TR-miR-17-92 cells (Mestdagh et al., 2009a) were cultured in RPMI (Invitrogen) supplemented with 10% fetal calf serum unless stated otherwise. SHEP-TR-miR-17-92 cells were treated with 2 μg/ml tetracycline (Sigma-Aldrich) to induce miR-17-92 expression (Figure S2A). TGF-β1 (PeproTech) and TGFBR1 inhibitor (SB431542, Sigma-Aldrich) were used at a concentration of 0.25 ng/ml and 2 μM, respectively, unless stated otherwise.

COFRADIC Analysis

SHEP-TR-miR-17-92 cells were metabolically labeled by growing them in DMEM medium supplemented with dialyzed fetal calf serum and with either heavy lysine and arginine (both $^{13}C_6$) or with natural, light lysine and arginine ($^{12}C_6$). This stable isotope labeling (SILAC [Ong et al., 2002]) ensures that following trypsin digestion, all generated peptides can be quantified by mass spectrometry (MS, see Supplemental Information). Mass spectrometry data for the forward en reverse experiment are available in Tables S4 and S5 and in the PRIDE database (http://www.ebi.ac.uk/pride; Accession number 14860).

mRNA and miRNA Expression Quantification

See Supplemental Information for details on mRNA and miRNA quantification and data normalization. miRNA expression data are available in rdml format (Document S2) (Lefever et al., 2009).

Immunohistochemistry and Western Blot

Briefly, SHEP-TR-miR-17-92 cells, tetracycline treated or untreated, were stimulated with TGF-β1 for 4 hr. pSMAD2 activity was evaluated by immunochemistry on cytopreparations or by western blot. See Supplemental Information for detailed experimental procedures.

Cell Adhesion and Proliferation Assays

Details on cell adhesion and proliferation assays are described in the Supplemental Information.

Xenografts

SHEP-TR-miR-17-92 and SHEP-TR (control) cells were transfected with a luciferase expressing mammalian vector. Etherotopic xenografts were established in atymic nude mice (n = 5) by injection of 10^6 SHEP-TR cells subcutaneosly in the left flanking site and 10^6 SHEP-TR-miR-17-92 cells in the right flanking site of each individual animal. See Supplemental Information for detailed experimental procedures.

CAGA-Luciferase Reporter Assay

For luciferase experiments, tetracycline or control treated SHEP-TR-miR-17-92 cells were transfected with the $(CAGA)_{12}$-Luc luciferase reporter vector and assayed for luciferase and renilla activity. See Supplemental Information for detailed experimental procedures.

3′UTR Reporter Assay

DLD1Dicer^{hypo} cells were seeded in DMEM (Invitrogen) supplemented with fetal calf serum (10%) at a density of 10,000 cells per well in an opaque 96-well plate. Twenty-four hours after seeding, using DharmaFECT Duo (Dharmacon), cells were cotransfected, either with a combination of a 3′UTR containing pGL4.11[luc2p] vector (Switchgear Genomics), a pRL-TK vector (Promega) for normalization, and a miR-17-92 pre-miR (Ambion) (10 nM) or with a combination of a psi-check2 vector (Promega) containing only part of the 3′UTR and a miR-17-92 pre-miR. Forty-eight hours after transfection, luciferase reporter gene activity was measured using the Dual-Glo Luciferase Assay System (Promega) and a FLUOstar OPTIMA microplate reader (BMG LABTECH). See Supplemental Information for details on plasmid construction and miRNA binding site mutation.

Statistics

See Supplemental Information for details on all statistical procedures and gene set enrichment analysis.

ACCESSION NUMBERS

The Gene Expression Omnibus accession number for the mRNA expression data reported in this paper is GSE21713. The PRIDE accession number for the protein expression data reported in this paper is 14860.

SUPPLEMENTAL INFORMATION

Supplemental Information includes seven figures, five tables, Supplemental Experimental Procedures, Supplemental References, and an RDML file for

(E) Relative 3′UTR luciferase reporter activity for TGFBR2, SMAD2, and SMAD4, measured in DLD1DICER^{hypo} cells (mean ± SEM). Plasmids with a wild-type seed site for the active miRNA were introduced in DLD1DICER^{hypo} cells in combination with a pre-miR negative control (NC) or miR-17-92 pre-miR. Luciferase activity is decreased significantly in the presence of the active miRNA (*) (t test, $p < 0.01$) and increases significantly when the seed for the active miRNA is mutated (MUT) (t test, $p < 0.01$).

RT-qPCR profiling and can be found with this article online at doi:10.1016/j.molcel.2010.11.038.

ACKNOWLEDGMENTS

This research was funded by the Fund for Scientific Research (grant number: G.0198.08 and 31511809), the Belgian Kid's Fund, and the Stichting tegen Kanker. P.M. is supported by the Ghent University Research Fund (BOF 01D31406). A.-K. B., K.S., and H.A. are supported by grants from the Swedish Childhood Cancer Foundation and the Swedish Cancer Society. E.F. is supported by The Royal Swedish Physiographic Society and the American Cancer Society. B.G. is a Postdoctoral Research Fellow for the Fund for Scientific Research- Flanders (Belgium). The VIB/UGent lab further acknowledges support by a research grant from the Fund for Scientific Research- Flanders (Belgium) (project numbers G.0077.06), the Concerted Research Actions (project BOF07/GOA/012) from the Ghent University, and the Inter University Attraction Poles (IUAP06). NCI grants R01 CA122334 and P30 CA016520 were to A.T.-T., and FP7-Tumic HEALTH-F2-2008-201662, Associazione Italiana contro la lotta al Neuroblastoma "Progetto Pensiero" and AIRC Tumori Pediatrici 2007-2010 to M.Z. G.V.P. was supported by a BOF research grant (01D35609). This article represents research results of the Belgian program of Interuniversity Poles of Attraction, initiated by the Belgian State, Prime Minister's Office, Science Policy Programming. The study was sponsored by the GOA (01G01910).

Received: April 22, 2010
Revised: October 6, 2010
Accepted: November 22, 2010
Published: December 9, 2010

REFERENCES

Baek, D., Villén, J., Shin, C., Camargo, F.D., Gygi, S.P., and Bartel, D.P. (2008). The impact of microRNAs on protein output. Nature *455*, 64–71.

Bartel, D.P. (2004). MicroRNAs: genomics, biogenesis, mechanism, and function. Cell *116*, 281–297.

Bartel, D.P. (2009). MicroRNAs: target recognition and regulatory functions. Cell *136*, 215–233.

Calin, G.A., and Croce, C.M. (2006). MicroRNA signatures in human cancers. Nat. Rev. Cancer *6*, 857–866.

Castellano, L., Giamas, G., Jacob, J., Coombes, R.C., Lucchesi, W., Thiruchelvam, P., Barton, G., Jiao, L.R., Wait, R., Waxman, J., et al. (2009). The estrogen receptor-alpha-induced microRNA signature regulates itself and its transcriptional response. Proc. Natl. Acad. Sci. USA *106*, 15732–15737.

Cohen, P.S., Letterio, J.J., Gaetano, C., Chan, J., Matsumoto, K., Sporn, M.B., and Thiele, C.J. (1995). Induction of transforming growth factor beta 1 and its receptors during all-trans-retinoic acid (RA) treatment of RA-responsive human neuroblastoma cell lines. Cancer Res. *55*, 2380–2386.

Colaert, N., Helsens, K., Impens, F., Vandekerckhove, J., and Gevaert, K. (2010). Rover: a tool to visualize and validate quantitative proteomics data from different sources. Proteomics *10*, 1226–1229.

Dews, M., Fox, J.L., Hultine, S., Sundaram, P., Wang, W., Liu, Y.Y., Furth, E., Enders, G.H., El-Deiry, W., Schelter, J.M., et al. (2010). The myc-miR-17∼92 axis blunts TGFbeta signaling and production of multiple TGFbeta-dependent antiangiogenic factors. Cancer Res. *70*, 8233–8246.

Dews, M., Homayouni, A., Yu, D., Murphy, D., Sevignani, C., Wentzel, E., Furth, E.E., Lee, W.M., Enders, G.H., Mendell, J.T., and Thomas-Tikhonenko, A. (2006). Augmentation of tumor angiogenesis by a Myc-activated microRNA cluster. Nat. Genet. *38*, 1060–1065.

Esquela-Kerscher, A., and Slack, F.J. (2006). Oncomirs - microRNAs with a role in cancer. Nat. Rev. Cancer *6*, 259–269.

Fontana, L., Fiori, M.E., Albini, S., Cifaldi, L., Giovinazzi, S., Forloni, M., Boldrini, R., Donfrancesco, A., Federici, V., Giacomini, P., et al. (2008). Antagomir-17-5p abolishes the growth of therapy-resistant neuroblastoma through p21 and BIM. PLoS ONE *3*, e2236.

Fredlund, E., Ringnér, M., Maris, J.M., and Påhlman, S. (2008). High Myc pathway activity and low stage of neuronal differentiation associate with poor outcome in neuroblastoma. Proc. Natl. Acad. Sci. USA *105*, 14094–14099.

Friedman, R.C., Farh, K.K., Burge, C.B., and Bartel, D.P. (2009). Most mammalian mRNAs are conserved targets of microRNAs. Genome Res. *19*, 92–105.

Gevaert, K., Van Damme, J., Goethals, M., Thomas, G.R., Hoorelbeke, B., Demol, H., Martens, L., Puype, M., Staes, A., and Vandekerckhove, J. (2002). Chromatographic isolation of methionine-containing peptides for gel-free proteome analysis: identification of more than 800 Escherichia coli proteins. Mol. Cell. Proteomics *1*, 896–903.

Hayashita, Y., Osada, H., Tatematsu, Y., Yamada, H., Yanagisawa, K., Tomida, S., Yatabe, Y., Kawahara, K., Sekido, Y., and Takahashi, T. (2005). A polycistronic microRNA cluster, miR-17-92, is overexpressed in human lung cancers and enhances cell proliferation. Cancer Res. *65*, 9628–9632.

He, L., Thomson, J.M., Hemann, M.T., Hernando-Monge, E., Mu, D., Goodson, S., Powers, S., Cordon-Cardo, C., Lowe, S.W., Hannon, G.J., and Hammond, S.M. (2005). A microRNA polycistron as a potential human oncogene. Nature *435*, 828–833.

He, L., He, X., Lim, L.P., de Stanchina, E., Xuan, Z., Liang, Y., Xue, W., Zender, L., Magnus, J., Ridzon, D., et al. (2007). A microRNA component of the p53 tumour suppressor network. Nature *447*, 1130–1134.

Lanza, G., Ferracin, M., Gafà, R., Veronese, A., Spizzo, R., Pichiorri, F., Liu, C.G., Calin, G.A., Croce, C.M., and Negrini, M. (2007). mRNA/microRNA gene expression profile in microsatellite unstable colorectal cancer. Mol. Cancer *6*, 54.

Laping, N.J., Grygielko, E., Mathur, A., Butter, S., Bomberger, J., Tweed, C., Martin, W., Fornwald, J., Lehr, R., Harling, J., et al. (2002). Inhibition of transforming growth factor (TGF)-beta1-induced extracellular matrix with a novel inhibitor of the TGF-beta type I receptor kinase activity: SB-431542. Mol. Pharmacol. *62*, 58–64.

Lefever, S., Hellemans, J., Pattyn, F., Przybylski, D.R., Taylor, C., Geurts, R., Untergasser, A., and Vandesompele, J.; RDML consortium. (2009). RDML: structured language and reporting guidelines for real-time quantitative PCR data. Nucleic Acids Res. *37*, 2065–2069.

Lovén, J., Zinin, N., Wahlström, T., Müller, I., Brodin, P., Fredlund, E., Ribacke, U., Pivarcsi, A., Påhlman, S., and Henriksson, M. (2010). MYCN-regulated microRNAs repress estrogen receptor-alpha (ESR1) expression and neuronal differentiation in human neuroblastoma. Proc. Natl. Acad. Sci. USA *107*, 1553–1558.

Mestdagh, P., Fredlund, E., Pattyn, F., Schulte, J.H., Muth, D., Vermeulen, J., Kumps, C., Schlierf, S., De Preter, K., Van Roy, N., et al. (2009a). MYCN/c-MYC-induced microRNAs repress coding gene networks associated with poor outcome in MYCN/c-MYC-activated tumors. Oncogene *29*, 1394–1404.

Mestdagh, P., Van Vlierberghe, P., De Weer, A., Muth, D., Westermann, F., Speleman, F., and Vandesompele, J. (2009b). A novel and universal method for microRNA RT-qPCR data normalization. Genome Biol. *10*, R64.

O'Donnell, K.A., Wentzel, E.A., Zeller, K.I., Dang, C.V., and Mendell, J.T. (2005). c-Myc-regulated microRNAs modulate E2F1 expression. Nature *435*, 839–843.

Oberthuer, A., Berthold, F., Warnat, P., Hero, B., Kahlert, Y., Spitz, R., Ernestus, K., König, R., Haas, S., Eils, R., et al. (2006). Customized oligonucleotide microarray gene expression-based classification of neuroblastoma patients outperforms current clinical risk stratification. J. Clin. Oncol. *24*, 5070–5078.

Olive, V., Bennett, M.J., Walker, J.C., Ma, C., Jiang, I., Cordon-Cardo, C., Li, Q.J., Lowe, S.W., Hannon, G.J., and He, L. (2009). miR-19 is a key oncogenic component of mir-17-92. Genes Dev. *23*, 2839–2849.

Ong, S.E., Blagoev, B., Kratchmarova, I., Kristensen, D.B., Steen, H., Pandey, A., and Mann, M. (2002). Stable isotope labeling by amino acids in cell culture,

SILAC, as a simple and accurate approach to expression proteomics. Mol. Cell. Proteomics *1*, 376–386.

Padua, D., Zhang, X.H., Wang, Q., Nadal, C., Gerald, W.L., Gomis, R.R., and Massagué, J. (2008). TGFbeta primes breast tumors for lung metastasis seeding through angiopoietin-like 4. Cell *133*, 66–77.

Petrocca, F., Visone, R., Onelli, M.R., Shah, M.H., Nicoloso, M.S., de Martino, I., Iliopoulos, D., Pilozzi, E., Liu, C.G., Negrini, M., et al. (2008). E2F1-regulated microRNAs impair TGFbeta-dependent cell-cycle arrest and apoptosis in gastric cancer. Cancer Cell *13*, 272–286.

Raver-Shapira, N., Marciano, E., Meiri, E., Spector, Y., Rosenfeld, N., Moskovits, N., Bentwich, Z., and Oren, M. (2007). Transcriptional activation of miR-34a contributes to p53-mediated apoptosis. Mol. Cell *26*, 731–743.

Scarpa, S., Coppa, A., Ragano-Caracciolo, M., Mincione, G., Giuffrida, A., Modesti, A., and Colletta, G. (1996). Transforming growth factor beta regulates differentiation and proliferation of human neuroblastoma. Exp. Cell Res. *229*, 147–154.

Schweigerer, L., Breit, S., Wenzel, A., Tsunamoto, K., Ludwig, R., and Schwab, M. (1990). Augmented MYCN expression advances the malignant phenotype of human neuroblastoma cells: evidence for induction of autocrine growth factor activity. Cancer Res. *50*, 4411–4416.

Selbach, M., Schwanhäusser, B., Thierfelder, N., Fang, Z., Khanin, R., and Rajewsky, N. (2008). Widespread changes in protein synthesis induced by microRNAs. Nature *455*, 58–63.

Subramanian, A., Tamayo, P., Mootha, V.K., Mukherjee, S., Ebert, B.L., Gillette, M.A., Paulovich, A., Pomeroy, S.L., Golub, T.R., Lander, E.S., and Mesirov, J.P. (2005). Gene set enrichment analysis: a knowledge-based approach for interpreting genome-wide expression profiles. Proc. Natl. Acad. Sci. USA *102*, 15545–15550.

Turco, A., Scarpa, S., Coppa, A., Baccheschi, G., Palumbo, C., Leonetti, C., Zupi, G., and Colletta, G. (2000). Increased TGFbeta type II receptor expression suppresses the malignant phenotype and induces differentiation of human neuroblastoma cells. Exp. Cell Res. *255*, 77–85.

Verrecchia, F., Chu, M.L., and Mauviel, A. (2001). Identification of novel TGF-beta /Smad gene targets in dermal fibroblasts using a combined cDNA microarray/promoter transactivation approach. J. Biol. Chem. *276*, 17058–17062.

Volinia, S., Calin, G.A., Liu, C.G., Ambs, S., Cimmino, A., Petrocca, F., Visone, R., Iorio, M., Roldo, C., Ferracin, M., et al. (2006). A microRNA expression signature of human solid tumors defines cancer gene targets. Proc. Natl. Acad. Sci. USA *103*, 2257–2261.

Xiao, C., Srinivasan, L., Calado, D.P., Patterson, H.C., Zhang, B., Wang, J., Henderson, J.M., Kutok, J.L., and Rajewsky, K. (2008). Lymphoproliferative disease and autoimmunity in mice with increased miR-17-92 expression in lymphocytes. Nat. Immunol. *9*, 405–414.

Zhang, H., Gao, P., Fukuda, R., Kumar, G., Krishnamachary, B., Zeller, K.I., Dang, C.V., and Semenza, G.L. (2007). HIF-1 inhibits mitochondrial biogenesis and cellular respiration in VHL-deficient renal cell carcinoma by repression of C-MYC activity. Cancer Cell *11*, 407–420.